Improved Design Optimization of Efficient Matching Networks for Capacitive Wireless Power Transfer Systems

Sreyam Sinha, Ashish Kumar and Khurram K. Afridi

Department of Electrical, Computer and Energy Engineering
University of Colorado Boulder
Boulder, USA
sreyam.sinha@colorado.edu; ashish.kumar@colorado.edu; khurram.afridi@colorado.edu

***Abstract*—Matching networks are an efficient means of providing large voltage and/or current gain and reactive compensation in high-frequency wireless power transfer (WPT) systems. This paper introduces an improved approach to designing matching networks for capacitive WPT systems, which maximizes the network efficiency while achieving the required overall gain and compensation. The proposed approach identifies the optimal number of matching network stages, the optimal distribution of gains and compensation among these stages, and the optimal air-gap voltage. The proposed approach is used to design the matching networks for a high-performance 6.78-MHz 250-W 1.2-cm air-gap prototype capacitive WPT system. The prototype system achieves a power transfer density of 51.4 kW/m^2 and an efficiency of 90.4%, which matches well with the theoretical prediction.**

Keywords—wireless power transfer; capacitive wireless power transfer; multistage matching network; L-section stage; high efficiency; voltage gain; current gain; compensation; design optimization

I. Introduction

Medium-range wireless power transfer (WPT) systems generally utilize magnetically coupled inductive coils to transfer power across the air-gap. For flux guidance, these inductive WPT systems typically require expensive and fragile ferrite cores that incur substantial losses; limiting their frequency of operation, and hence, their potential for size reduction [1], [2]. On the other hand, capacitive WPT systems utilize electrically coupled conductive plates for power transfer. Since capacitive WPT systems do not require ferrites, they can be operated at high frequencies, reducing their size and cost. Hence, capacitive WPT systems can be an attractive alternative for a variety of applications [3]-[7], including electric vehicle (EV) charging [8]-[14]. To achieve high efficiencies and high power transfer densities, while maintaining fringing electric fields within safe limits [15], capacitive WPT systems require circuit stages that provide appropriate voltage and/or current gain as well as reactive compensation. Matching networks are an efficient means of providing the required gain and compensation simultaneously [7]-[10], [16].

An approach that optimizes the design of multistage matching networks for capacitive WPT systems has recently been proposed in [16]. However, the design approach in [16] assumes a given number of matching network stages and a given air-gap voltage. This paper introduces an improved design approach that maximizes the matching network efficiency by identifying the optimal number of stages, the optimal distribution of gains and compensations among these stages, and the optimal air-gap voltage. A prototype 6.78-MHz 250-W 1.2-cm air-gap capacitive WPT system with 25-cm^2 coupling plates, utilizing matching networks designed using the proposed approach, is built and tested. The matching networks enable this prototype system to achieve a power transfer density of 51.4 kW/m^2 and an efficiency of 90.4%, which is in good agreement with the theoretical prediction.

The remainder of this paper is organized as follows: Section II introduces the proposed approach to optimizing the design of matching networks for capacitive WPT systems. Section III

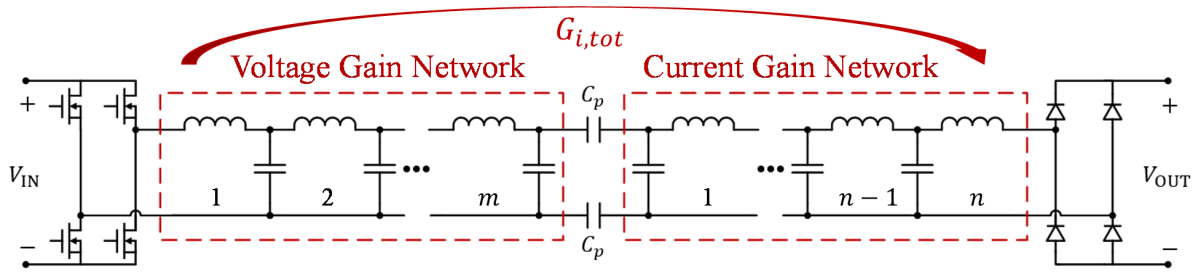

Fig. 1. A capacitive WPT system with gain and compensation networks implemented using multistage L-section matching networks.

presents the optimization results and draws insights regarding the optimal number of matching network stages and the optimal distribution of gains and compensation among these stages. Experimental results validating the proposed design approach are presented in Section IV. Finally, Section V summarizes and concludes the paper.

II. Proposed Matching Network Design Approach

A capacitive WPT system utilizing multistage L-section matching networks is shown in Fig. 1. In this system, two pairs of conductive plates (shown as C_p) separated by air-gaps are utilized to achieve wireless power transfer. The inverter converts the dc input voltage into high-frequency ac, which is stepped up by a voltage gain network to enable high power transfer with low displacement current through the air-gap. This results in a relatively low voltage across the air-gap, and hence, low fringing fields, which helps meet field safety requirements. The current gain network on the other side of the coupling plates steps the ac current back up (and the voltage down) to the level required at the output. The voltage gain and current gain networks also compensate for the capacitive reactance of the coupling plates.

Consider the multistage matching networks in the capacitive WPT system of Fig. 1. Each L-section stage of these networks can be characterized in terms of three quantities: G_i, the current gain provided by the L-section stage, defined as $G_i = \frac{|\hat{I}_{out}|}{|\hat{I}_{in}|}$, where $|\hat{I}_{out}|$ and $|\hat{I}_{in}|$ are the amplitudes of the output and input currents of the stage, respectively; Q_{load}, the load impedance characteristic of the L-section stage, defined as $Q_{load} = \frac{X_{load}}{R_{load}}$, where X_{load} and R_{load} are the imaginary and real parts of the load impedance of the stage, respectively; and Q_{in}, the input impedance characteristic of the L-section stage, defined as $Q_{in} = \frac{X_{in}}{R_{in}}$, where X_{in} and R_{in} are the imaginary and real parts of the input impedance of the stage, respectively. These quantities are illustrated in Fig. 2 for an L-section voltage gain stage and an L-section current gain stage. Note that while G_i is a measure of the gain, Q_{in} and Q_{load} are measures of the compensation provided by an L-section stage.

Given the required values of G_i, Q_{load}, Q_{in} and R_{load} for each L-section stage of the voltage gain network of the capacitive WPT system of Fig. 1, the inductance and capacitance values of the stage can be determined using the following expressions:

$$L = \frac{\left(G_i\sqrt{(1-G_i^2)+Q_{load}^2}+G_i^2 Q_{in}\right)R_{load}}{2\pi f_S},$$
$$C = \frac{1-G_i^2}{2\pi f_S\left(G_i\sqrt{(1-G_i^2)+Q_{load}^2}-G_i^2 Q_{load}\right)R_{load}}. \quad (1)$$

Similarly, the expressions for the inductance and the capacitance values for each L-section stage of the current gain network of the capacitive WPT system of Fig. 1 are given by:

$$L = \frac{\left(\sqrt{(G_i^2-1)+G_i^2 Q_{in}^2}-Q_{load}\right)R_{load}}{2\pi f_S},$$

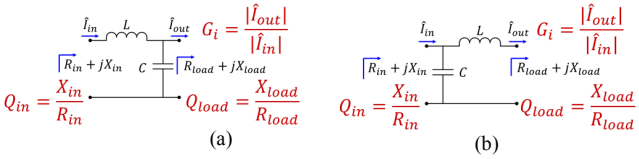

Fig. 2. Two types of L-section stages utilized in the multistage matching networks of the capacitive WPT system of Fig. 1: (a) voltage gain stage and (b) current gain stage.

TABLE I. Expressions for the Effective Transformation Factor Q_{eff} for the L-section stages of Fig. 2

L-section Stage Type	Expression for Q_{eff}
Voltage gain (Fig. 2(a))	$\frac{1}{G_i}\sqrt{1-G_i^2+Q_{load}^2}+Q_{in}$
Current gain (Fig. 2(b))	$G_i\sqrt{1-\frac{1}{G_i^2}+Q_{in}^2}-Q_{load}$

$$C = \frac{1-\frac{1}{G_i^2}}{2\pi f_S\left(\sqrt{(G_i^2-1)+G_i^2 Q_{in}^2}+Q_{in}\right)R_{load}}. \quad (2)$$

Assuming that an L-section stage is highly efficient, and that the losses in its capacitor can be neglected in comparison to the losses in its inductor, the efficiency of the stage can be expressed as:

$$\eta \approx 1 - \frac{Q_{eff}}{Q_L}. \quad (3)$$

Here, Q_{eff} is an effective transformation factor associated with the L-section stage, and Q_L is the inductor quality factor. The effective transformation factor Q_{eff} is a function of the current gain (G_i) and the input and load impedance characteristics (Q_{in} and Q_{load}) of the stage, and hence, encapsulates both the gain and the compensation provided by the stage. Expressions for this effective transformation factor for the voltage gain and current gain stages shown in Fig. 2 are provided in Table I, and their derivations can be found in [16]. Using (3), the overall matching network efficiency in the capacitive WPT system of Fig. 1 with m stages in the voltage gain network and n stages in the current gain network can be approximated as:

$$\eta_{multistage,m-n} \approx 1 - \frac{\sum_{p=1}^{m} Q_{eff,VG,p}+\sum_{q=1}^{n} Q_{eff,CG,q}}{Q_L}, \quad (4)$$

where $Q_{eff,VG,p}$ and $Q_{eff,CG,q}$ are the effective transformation factors of the p-th and q-th stages of the voltage gain and current gain network, respectively. A derivation of the efficiency expression given in (4) is provided in Appendix A.

Maximizing the overall matching network efficiency in the capacitive WPT system of Fig. 1 requires the selection of the optimal number of voltage gain and current gain stages, and the optimal distribution of current gains (G_i's) and compensation (i.e., appropriate values of Q_{in}'s and Q_{load}'s) among these stages. The capacitive WPT system of Fig. 1 enforces five design constraints on this optimization. First, the total current gain of the overall matching network, $G_{i,tot}$ (as shown in Fig 1), is constrained by the specified input and output voltages (V_{IN} and V_{OUT}, respectively) of the WPT system. Second, to ensure

that the L-section stages of the voltage gain network are physically realizable (that is, their inductance and capacitance values are non-negative), each stage of the voltage gain network must provide a current gain smaller than or equal to 1. Similarly, each stage of the current gain network must provide a current gain larger than or equal to 1. Third, the impedance seen by the inverter has to be near-resistive to maintain zero-voltage switching (ZVS) and near-zero-current switching (near-ZCS) of the inverter transistors. Fourth, the impedance looking into the rectifier is resistive under fundamental frequency analysis. Finally, the load impedance characteristic of the last voltage gain stage ($Q_{load,VG,m}$) and the input impedance characteristic of the first current gain stage ($Q_{in,CG,1}$) are related by the reactance of the coupling plates, X_p ($= -\frac{1}{2\pi f_s C_p}$, where f_s is the operating frequency of the capacitive WPT system). With these constraints, the optimization problem can be formally expressed as:

$$\max\ \eta_{multistage,m-n}, \tag{5a}$$

subject to:

$$\prod_{p=1}^{m} G_{i,VG,p} \prod_{q=1}^{n} G_{i,CG,q} = G_{i,tot},$$

$$G_{i,VG,p} \le 1\ \forall\ p = 1,2,\dots,m, \quad G_{i,CG,q} \ge 1\ \forall\ q = 1,2,\dots,n,$$

$$Q_{in,VG,1} = 0,$$

$$Q_{load,CG,n} = 0,$$

$$Q_{in,CG,1} - Q_{load,VG,m} = K_{sys} \prod_{p=1}^{m} G_{i,VG,p}^2. \tag{5b}$$

Here, $G_{i,VG,p}$ is the current gain provided by the p-th voltage gain stage, $G_{i,CG,q}$ is the current gain provided by the q-th current gain stage, $Q_{in,VG,1}$ is the input impedance characteristic of the first voltage gain stage, $Q_{load,CG,n}$ is the load impedance characteristic of the last current gain stage, and K_{sys} is a constant associated with the system, given by: $K_{sys} = \frac{4|X_p|P_{\mathrm{OUT}}}{k_{inv}^2 V_{\mathrm{IN}}^2}$, where P_{OUT} is the output power, and k_{inv} is the voltage gain associated with the inverter, which depends on the inverter's topology and is equal to $\frac{4}{\pi}$ for the full-bridge inverter of Fig. 1. This constrained optimization problem is solved using the method of Lagrange multipliers, and its results are discussed below.

III. Optimization Results and Insights

When the above-described methodology is applied to the capacitive WPT system of Fig. 1, the following results are obtained. In the optimized design, the current gains (G_i's) provided by the first $m-1$ stages of the voltage gain network come out to be equal (denoted by $G_{i,VG,eq}$), that is:

$$G_{i,VG,1} = G_{i,VG,2} = \cdots = G_{i,VG,m-1} \overset{\text{def}}{=} G_{i,VG,eq}. \tag{6}$$

This optimal equal current gain $G_{i,VG,eq}$ can be found by solving the following equation:

$$1 + G_{i,VG,eq}^2 = \begin{cases} \max[F_{v1}, F_{v2}, F_{v3}], & \text{if } n \ge 1, \\ \dfrac{G_{i,VG,eq}^{2m-1}\left(1+K_{sys}^2 G_{i,tot}^4\right)}{G_{i,tot}\sqrt{G_{i,VG,eq}^{2(m-1)}\left(1+K_{sys}^2 G_{i,tot}^4\right) - G_{i,tot}^2}}, & \text{if } n = 0, \end{cases} \tag{7}$$

where:

$$F_{v1} = \frac{K_{sys} G_{i,tot} G_{i,VG,eq}^{(m+n-1)}}{\sqrt{K_{sys} G_{i,tot} G_{i,VG,eq}^{m+n-2} - 1}},$$

$$F_{v2} = \frac{2K_{sys}(m-1) G_{i,tot} G_{i,VG,eq}^{3m-n-2} - (m-n)\left(G_{i,VG,eq}^{2(m-n)} + G_{i,tot}^2\right)}{(m+n-2) G_{i,tot} G_{i,VG,eq}^{m-n-1}}, \text{ and}$$

$$F_{v3} = \frac{2K_{sys}(n-1) G_{i,tot}^3 G_{i,VG,eq}^{m+n-2} + (m-n)\left(G_{i,VG,eq}^{2(m-n)} + G_{i,tot}^2\right)}{(m+n-2) G_{i,tot} G_{i,VG,eq}^{m-n-1}}.$$

The optimal current gains of the last $n-1$ stages of the current gain network are also found to be equal (denoted by $G_{i,CG,eq}$), that is:

$$G_{i,VG,m} = \begin{cases} \sqrt{\dfrac{1}{K_{sys}}\left(\dfrac{G_{i,VG,eq}^{1-m} G_{i,CG,eq}^{n-1}}{G_{i,tot}} + \dfrac{G_{i,tot}}{G_{i,VG,eq}^{3(m-1)} G_{i,CG,eq}^{n-1}}\right)}, & \text{if } n \ge 1 \text{ and } F_{v1} = \max[F_{v1}, F_{v2}, F_{v3}], \\ 1, & \text{if } n \ge 1 \text{ and } F_{v2} = \max[F_{v1}, F_{v2}, F_{v3}], \\ \dfrac{G_{i,tot}}{G_{i,VG,eq}^{m-1} G_{i,CG,eq}^{n-1}}, & \text{if } n \ge 1 \text{ and } F_{v3} = \max[F_{v1}, F_{v2}, F_{v3}], \\ \dfrac{G_{i,tot}}{G_{i,VG,eq}^{m-1}}, & \text{if } n = 0. \end{cases} \tag{10}$$

$$G_{i,CG,1} = \begin{cases} \sqrt{\dfrac{K_{sys} G_{i,tot}^2}{\left(\dfrac{G_{i,VG,eq}^{m-1} G_{i,CG,eq}^{3(n-1)}}{G_{i,tot}} + \dfrac{G_{i,tot}}{G_{i,VG,eq}^{m-1} G_{i,CG,eq}^{1-n}}\right)}}, & \text{if } m \ge 1 \text{ and } F_{c1} = \min[F_{c1}, F_{c2}, F_{c3}], \\ \dfrac{G_{i,tot}}{G_{i,VG,eq}^{m-1} G_{i,CG,eq}^{n-1}}, & \text{if } m \ge 1 \text{ and } F_{c2} = \min[F_{c1}, F_{c2}, F_{c3}], \\ 1, & \text{if } m \ge 1 \text{ and } F_{c3} = \min[F_{c1}, F_{c2}, F_{c3}], \\ \dfrac{G_{i,tot}}{G_{i,CG,eq}^{n-1}}, & \text{if } m = 0. \end{cases} \tag{11}$$

$$G_{i,CG,n} = G_{i,CG,n-1} = \cdots = G_{i,CG,2} \stackrel{\text{def}}{=} G_{i,CG,eq}. \quad (8)$$

This optimal equal current gain $G_{i,CG,eq}$ can be obtained by solving the following equation:

$$1 + G_{i,CG,eq}^2 = \begin{cases} \min[F_{c1}, F_{c2}, F_{c3}], & \text{if } m \geq 1, \\ \dfrac{G_{i,tot}^2(1+K_{sys}^2)}{G_{i,CG,eq}^{n-2}\sqrt{G_{i,tot}^2(1+K_{sys}^2) - G_{i,CG,eq}^{2(n-1)}}}, & \text{if } m = 0, \end{cases} \quad (9)$$

where:

$$F_{c1} = \frac{K_{sys} G_{i,tot} G_{i,CG,eq}^{\frac{4-m-n}{2}}}{\sqrt{K_{sys} G_{i,tot} - G_{i,CG,eq}^{m+n-2}}},$$

$$F_{c2} = \frac{2K_{sys}(m-1) G_{i,tot} G_{i,CG,eq}^{n-3m+2} - (m-n)\left(G_{i,CG,eq}^{2(n-m)} + G_{i,tot}^2\right)}{(m+n-2) G_{i,tot} G_{i,CG,eq}^{n-m-1}}, \text{ and}$$

$$F_{c3} = \frac{2K_{sys}(n-1) G_{i,tot}^3 G_{i,VG,eq}^{2-m-n} + (m-n)\left(G_{i,CG,eq}^{2(n-m)} + G_{i,tot}^2\right)}{(m+n-2) G_{i,tot} G_{i,CG,eq}^{n-m-1}}.$$

The optimal current gains of the remaining stages, that is, the last (m-th) stage of the voltage gain network ($G_{i,VG,m}$) and the first stage of the current gain network ($G_{i,CG,1}$) can then be found using (10) and (11), respectively, shown at the bottom of the previous page.

The optimal load impedance characteristics (Q_{load}'s) of the first $m-1$ voltage gain stages are also equal, and are related to the optimal equal current gain of these stages, $G_{i,VG,eq}$, as:

$$Q_{load,VG,1} = Q_{load,VG,2} = \cdots = Q_{load,VG,m-1} = -G_{i,VG.eq}. \quad (12)$$

The optimal load impedance characteristic of the last (m-th) voltage gain stage is given by (13), shown at the bottom of this page. Similarly, the optimal input impedance characteristics of the last $n-1$ stages of the current gain network are equal, and are related to the optimal equal current gain of these stages, $G_{i,CG,eq}$, as:

$$Q_{in,CG,n} = Q_{in,CG,n-1} = \cdots = Q_{in,CG,2} = \frac{1}{G_{i,CG.eq}}. \quad (14)$$

The optimal input impedance characteristic of the first current gain stage is given by (15), shown at the bottom of this page. The remaining compensation characteristics (Q_{in}'s and Q_{load}'s) can be found by noting that for a multistage network, the input impedance characteristic of a stage equals the load impedance characteristic of the preceding stage, i.e., $Q_{in,p} = Q_{load,p-1}$.

For a capacitive WPT system with a given number of voltage

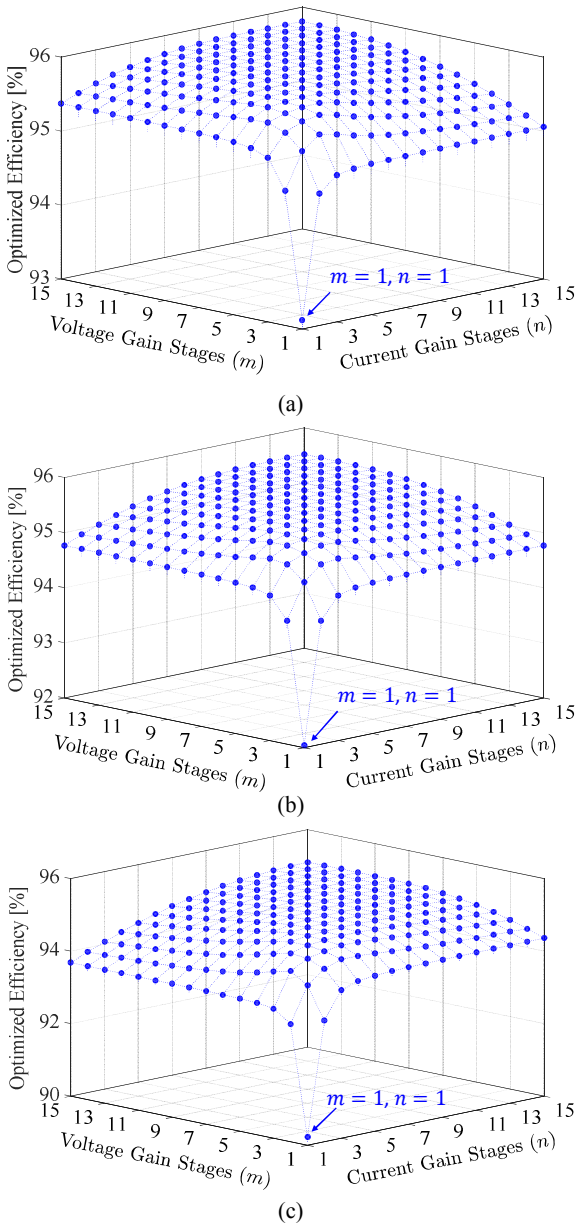

Fig. 3. Optimized matching network efficiency as a function of the number of voltage gain and current gain stages, for different values of total current gain: (a) $G_{i,tot} = 0.75$, (b) $G_{i,tot} = 1$, and (c) $G_{i,tot} = 1.5$.

$$Q_{load,VG,m} = \begin{cases} -\dfrac{G_{i,tot}}{G_{i,VG,eq}^{m-1} G_{i,CG,eq}^{n-1}}, & \text{if } n \geq 1 \text{ and } (F_{v1} = \max[F_{v1}, F_{v2}, F_{v3}] \text{ or } F_{v3} = \max[F_{v1}, F_{v2}, F_{v3}]), \\ \dfrac{G_{i,VG,eq}^{m-1} G_{i,CG,eq}^{n-1}}{G_{i,tot}} - K_{sys} G_{i,VG,eq}^{2(m-1)}, & \text{if } n \geq 1 \text{ and } F_{v2} = \max[F_{v1}, F_{v2}, F_{v3}], \\ -K_{sys} G_{i,tot}^2, & \text{if } n = 0. \end{cases} \quad (13)$$

$$Q_{in,CG,1} = \begin{cases} \dfrac{G_{i,VG,eq}^{m-1} G_{i,CG,eq}^{n-1}}{G_{i,tot}}, & \text{if } m \geq 1 \text{ and } (F_{c1} = \max[F_{c1}, F_{c2}, F_{c3}] \text{ or } F_{c2} = \min[F_{c1}, F_{c2}, F_{c3}]), \\ \dfrac{K_{sys} G_{i,tot}^2}{G_{i,CG,eq}^{2(n-1)}} - \dfrac{G_{i,tot}}{G_{i,VG,eq}^{m-1} G_{i,CG,eq}^{n-1}}, & \text{if } m \geq 1 \text{ and } F_{c3} = \min[F_{c1}, F_{c2}, F_{c3}], \\ K_{sys}, & \text{if } m = 0. \end{cases} \quad (15)$$

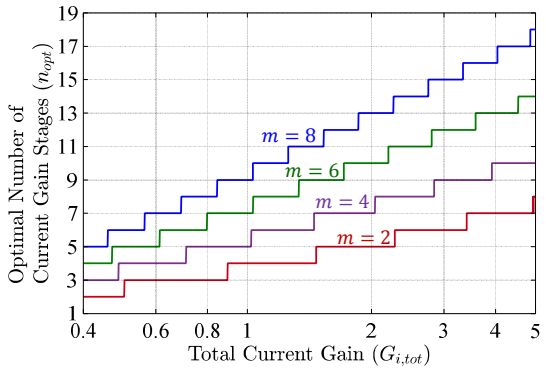

(a)

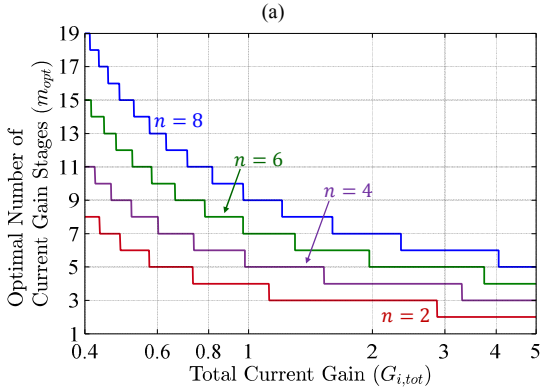

(b)

Fig. 4. Optimal number of stages for a 6.78-MHz 2-kW capacitive WPT system with a coupling capacitance of 20 pF, as a function of the total current gain $G_{i,tot}$: (a) optimal number of current gain stages n_{opt} for various values of the number of voltage gain stages m, and (b) optimal number of voltage gain stages m_{opt} for various values of the number of current gain stages n.

and current gain stages (m and n), the optimal current gains and compensation characteristics of all the stages can be determined using (6)-(15). Given these optimal current gains and compensation characteristics, the required inductance and capacitance values for each stage can be obtained using (1) and (2), and the optimized matching network efficiency can be determined using (4).

The optimized matching network efficiency for the capacitive WPT system of Fig. 1 is shown as a function of the number of stages in the voltage gain and the current gain networks, m and n, for three different values of the total current gain $G_{i,tot}$ in Fig. 3. Here, the capacitive WPT system operates at a switching frequency f_s of 6.78 MHz, output power P_{OUT} of 2 kW and input voltage V_{IN} of 300 V, with a coupling capacitance C_p of 20 pF (corresponding to 40 cm × 40 cm coupling plates separated by a 12-cm air-gap), and an inductor quality factor Q_L of 200. As can be seen, for each value of total current gain $G_{i,tot}$, when the voltage gain network has one stage ($m = 1$), the optimized efficiency increases monotonically with the number of current gain stages n. Similarly, when the current gain network has one stage ($n = 1$), the optimized efficiency increases monotonically with the number of voltage gain stages m. However, when the voltage gain network has multiple stages ($m > 1$), for each value of m, there is an optimal number of current gain stages n_{opt} at which the matching network efficiency is maximized. This optimal number of current gain stages n_{opt} is plotted as a function of the total current gain $G_{i,tot}$, for various values of the number of voltage gain stages m, in Fig. 4(a). It can be seen that for each value of m, as the required total current gain $G_{i,tot}$ increases, the optimal number of current gain stages n_{opt} also increases. Figure 3 also shows that when the current gain network has multiple stages ($n > 1$), for each value of the number of current gain stages n, there is an optimal number of voltage gain stages m_{opt}. This optimal number of voltage gain stages m_{opt} is shown as a function of the total current gain $G_{i,tot}$ for various values of the number of current gain stages n in Fig. 4(b). In this case, for each value of n, as the required total current gain $G_{i,tot}$ increases (and hence, the total voltage gain decreases), the optimal number of voltage gain stages m_{opt} becomes progressively smaller. It can also be seen from Fig. 4 that when the capacitive WPT system provides no net gain (that is, $G_{i,tot} = 1$), as the number of voltage gain and current gain stages (m and n) are increased, the optimal number of current gain stages n_{opt} approaches the number of voltage gain stages m (see Fig. 4(a)), and the optimal number of voltage gain stages m_{opt} approaches the number of current gain stages n (see Fig. 4(b)). Therefore, for capacitive WPT systems with a relatively large number of voltage gain and current gain stages and a total current gain of 1, symmetrical designs with equal number of voltage gain and current gain stages are the most efficient.

The proposed optimization methodology also determines the optimal air-gap voltage, given by:

$$v_{ag,opt} = \frac{P_{\text{OUT}}}{4\sqrt{2}V_{\text{IN}}f_s C_p}\prod_{p=1}^{m} G_{i,VG,p}. \tag{16}$$

As can be seen, the optimal air-gap voltage, and hence, the strength of fringing electric fields, reduces as the operating frequency increases.

IV. Experimental Validation

To validate the predictions of the proposed design approach, a 6.78-MHz 250-W capacitive WPT system with 5-cm × 5-cm coupling plates separated by a 1.2-cm air-gap (suitable as a single module of a multi-modular capacitive WPT system [6] for low-ground-clearance electric forklifts), and comprising single-stage voltage gain and current gain networks is designed, built and tested. A circuit schematic of the prototype system is

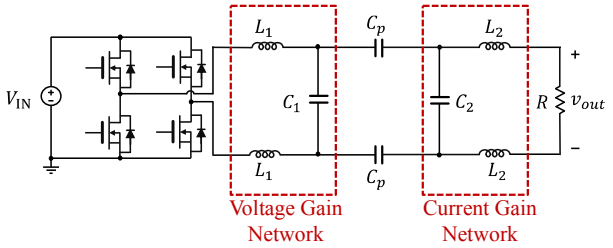

Fig. 5. Schematic of the prototype capacitive WPT system comprising single- stage voltage gain and current gain networks.

shown in Fig. 5, and a photograph of the system is shown in Fig. 6. The inverter in the prototype system is implemented using GaN Systems GS66506T enhancement-mode GaN transistors, and the rectifier and load are emulated using a 45 Ω resistor. The inductors in the prototype system have a quality factor of approximately 425. The measured switch-node voltages, inverter output current and load voltage waveforms of the prototype system while transferring 250 W are shown in Fig. 7. As can be seen, the impedance seen by the inverter is near-resistive, and sufficiently inductive to achieve zero-voltage switching of the inverter transistors. This prototype capacitive WPT system achieves a power transfer density of 51.4 kW/m^2. The measured efficiency of the prototype system (including the inverter) is 90.4%, and the measured matching network efficiency is 91.1%, which matches well with the theoretically predicted matching network efficiency of 91.5%.

V. Summary and Conclusions

This paper introduces an improved approach to designing matching networks for capacitive WPT systems, which maximizes network efficiency by identifying the optimal number of matching network stages, the optimal distribution of gains and compensation among these stages, and the optimal air-gap voltage. A 6.78-MHz, 250-W 1.2-cm air-gap prototype capacitive WPT system comprising matching networks designed using the proposed approach is built and tested. The prototype system achieves a power transfer density of 50 kW/m^2 and an efficiency of 90.4%, which matches well with the theoretical prediction.

Acknowledgment

The authors would like to acknowledge the Advanced Research Projects Agency – Energy (ARPA-E) for financially supporting this work under Award Number DE-AR0000618.

Appendix A

This appendix derives the expression for the overall matching network efficiency in the capacitive WPT system of Fig. 1, as given in (4). Consider the voltage gain network of the capacitive WPT system of Fig. 1. Assuming that the inductors in all the stages of this network have the same quality factor, the efficiency of the m-stage voltage gain network can be

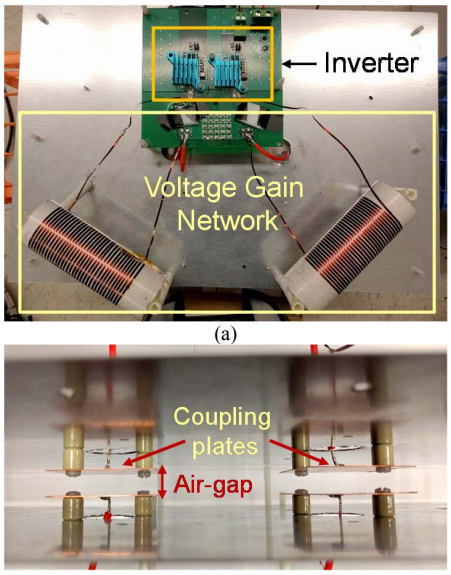

Fig. 6. (a) Primary-side view of the prototype test circuit with the inverter and the voltage gain network, and (b) coupling plates separated by 1.2 cm air-gap.

expressed as:

$$\eta_{VG} = \left(1 - \frac{Q_{eff,VG,1}}{Q_L}\right)\left(1 - \frac{Q_{eff,VG,1}}{Q_L}\right) \dots \left(1 - \frac{Q_{eff,VG,m}}{Q_L}\right). \quad (17)$$

Here, $Q_{eff,VG,p}$ is the effective transformation factor associated with the p-th stage of the voltage gain network. Assuming that all the stages of the network are highly efficient, the efficiency expression in (17) can be further approximated as:

$$\eta_{VG} \approx 1 - \frac{\sum_{p=1}^{m} Q_{eff,VG,p}}{Q_L}. \quad (18)$$

Similarly, the efficiency of the current gain network can be approximated as:

$$\eta_{CG} \approx 1 - \frac{\sum_{q=1}^{n} Q_{eff,CG,q}}{Q_L}. \quad (19)$$

The overall efficiency of this m - n multistage matching network is then given by:

$$\eta_{multistage,m-n} = \eta_{VG}\,\eta_{CG} \approx \left(1 - \frac{\sum_{p=1}^{m} Q_{eff,VG,p}}{Q_L}\right)\left(1 - \frac{\sum_{q=1}^{n} Q_{eff,CG,q}}{Q_L}\right). \quad (20)$$

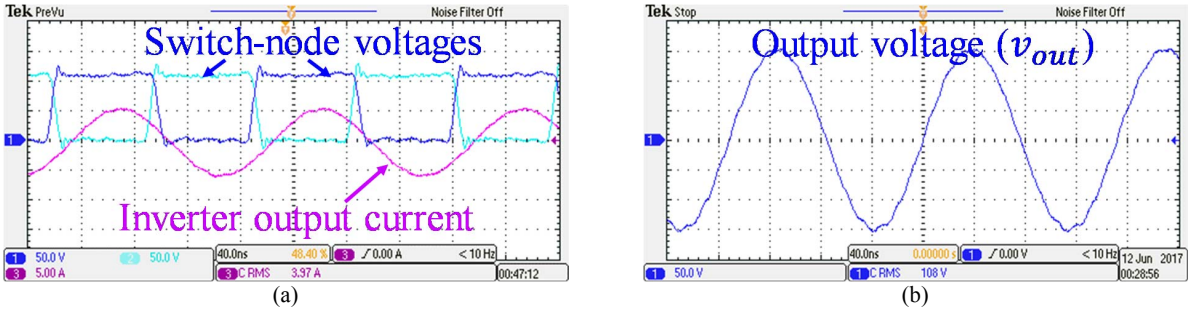

Fig. 7. Measured waveforms: (a) switch-node voltages and inverter output current, and (b) measured output voltage across 45 Ω load.

Invoking the high-efficiency assumption again, the overall matching network efficiency in the capacitive WPT system of Fig. 1, as expressed in (20), can be further approximated as:

$$\eta_{multistage,m-n} \approx 1 - \frac{\sum_{p=1}^{m} Q_{eff,VG,p} + \sum_{q=1}^{n} Q_{eff,CG,q}}{Q_L}. \quad (21)$$

REFERENCES

[1] G.A. Covic and J.T. Boys, "Modern Trends in Inductive Power Transfer for Transportation Applications," *IEEE Journal of Emerging and Selected Topics in Power Electronics,* vol. 1, no. 1, pp. 28-41, March 2013.

[2] S.Y.R. Hui, Wenxing Zhong and C.K. Lee, "A Critical Review of cent Progress in Mid-Range Wireless Power Transfer," *IEEE Transactions on Power Electronics*, vol. 29, no. 9, pp. 4500-4511, September 2014.

[3] A.M. Sodagar and P. Amiri, "Capacitive coupling for power and data telemetry to implantable biomedical microsystems," *Proceedings of the IEEE/EMBS International Conference on Neural Engineering (NER)*, pp. 411-414, Antalya, Turkey, April-May 2009.

[4] M. Kline, I. Izyumin, B. Boser and S. Sanders, "Capacitive Power Transfer for Contactless Charging," *Proceedings of the IEEE Applied Power Electronics Conference and Exposition (APEC)*, pp. 1398-1404, Fort Worth, TX, March 2011.

[5] M. P. Theodoridis, "Effective Capacitive Power Transfer," *IEEE Transactions on Power Electronics*, vol. 27, no. 12, pp. 4906-4913, December 2012.

[6] A. Kumar, S. Pervaiz, C.K. Chang, S. Korhummel, Z. Popovic and K.K. Afridi, "Investigation of Power Transfer Density Enhancement in Large Air-Gap Capacitive Wireless Power Transfer Systems," *Proceedings of the IEEE Wireless Power Transfer Conference (WPTC)*, Boulder, CO, May 2015.

[7] S. Sinha, A. Kumar and K.K. Afridi, "Active Variable Reactance Rectifier – A New Approach to Compensating for Coupling Variations in Wireless Power Transfer Systems," *Proceedings of the IEEE Workshop on Control and Modeling for Power Electronics (COMPEL)*, Stanford, CA, July 2017.

[7] F. Lu, H. Zhang, H. Hofmann and C. Mi, "A Double-Sided LCLC-Compensated Capacitive Power Transfer System for Electric Vehicle Charging," *IEEE Transactions on Power Electronics*, vol. 30, no. 11, pp. 6011-6014, November 2015.

[8] F. Lu, H. Zhang, H. Hofmann and C. Mi, "A CLLC-compensated high power and large air-gap capacitive power transfer system for electric vehicle charging applications," *Proceedings of the IEEE Applied Power Electronics Conference and Exposition (APEC)*, Long Beach, CA, March 2016.

[9] H. Zhang, F. Lu, H. Hofmann, W. Liu and C.C. Mi, "A Four-Plate Compact Capacitive Coupler Design and LCL-Compensated Topology for Capacitive Power Transfer in Electric Vehicle Charging Application," *IEEE Transactions on Power Electronics*, vol. 31, no. 12, pp. 8541-8551, December 2016.

[10] F. Lu, H. Zhang, H. Hofmann and C.C. Mi, "An Inductive and Capacitive Combined Wireless Power Transfer System With LC-Compensated Topology," *IEEE Transactions on Power Electronics*, vol. 31, no. 12, pp. 8471-8482, December 2016.

[11] I. Ramos, K.K. Afridi, J. Estrada and Z. Popovic, "Near-field Capacitive Wireless Power Transfer Array with External Field Cancellation," *Proceedings of the IEEE Wireless Power Transfer Conference (WPTC)*, Aveiro, Portugal, May 2016.

[12] B. Regensburger, A. Kumar, S. Sinha, K. Doubleday, S. Pervaiz, Z. Popovic and K.K. Afridi, "High-Performance Large Air-Gap Capacitive Wireless Power Transfer System for Electric Vehicle Charging," *Proceedings of the IEEE Transportation Electrification Conference & Exposition (ITEC)*, Chicago, IL, June 2017.

[13] K. Doubleday, S. Sinha, B. Regensburger, S. Pervaiz, A. Kumar and K.K. Afridi, "Design Tradeoffs in a Multi-Modular Capacitive Wireless Power Transfer System," *Proceedings of the IEEE Workshop on Emerging Technologies: Wireless (WoW)*, Knoxville, TN, October 2016.

[14] S. Sinha, B. Regensburger, K. Doubleday, A. Kumar, S. Pervaiz and K.K. Afridi, "High-Power-Transfer-Density Capacitive Wireless Power Transfer System for Electric Vehicle Charging," *Proceedings of the IEEE Energy Conversion Congress and Exposition (ECCE)*, Cincinnati, OH, October 2017.

[15] International Commission on Non-Ionizing Radiation Protection, "ICNIRP Guidelines for Limiting Exposure to Time-Varying Electric, Magnetic and Electromagnetic Fields (up to 300 GHz)," *Health Physics*, vol. 99, no. 6, pp. 818–836, December 2010.

[16] S. Sinha, A. Kumar, S. Pervaiz, B. Regensburger and K.K. Afridi, "Design of Efficient Matching Networks for Capacitive Wireless Power Transfer Systems," *Proceedings of the IEEE Workshop on Control and Modeling for Power Electronics (COMPEL)*, Trondheim, Norway, June 2016.